Article

Simple Cubic Super Crystals Containing PbTe Nanocubes and Their Core#Shell Building Blocks

Jun Zhang, Amar Kumbhar, Jibao He, Narayan Chandra Das, Kaikun Yang, Jian-Qing Wang, Howard Wang, Kevin L. Stokes, and Jiye Fang

J. Am. Chem. Soc., **2008**, 130 (45), 15203-15209 • DOI: 10.1021/ja806120w • Publication Date (Web): 21 October 2008

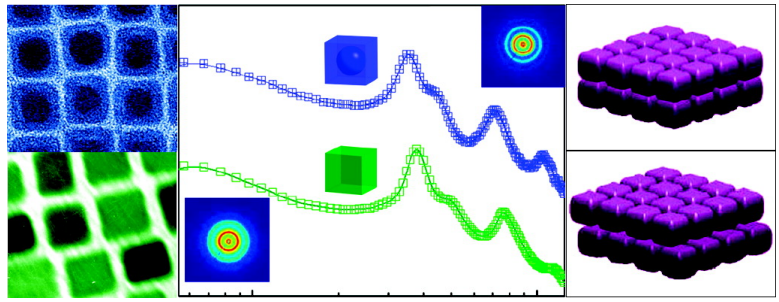

J|A|C|S
ARTICLES

Published on Web 10/21/2008

Simple Cubic Super Crystals Containing PbTe Nanocubes and Their Core−Shell Building Blocks

Jun Zhang,[†] Amar Kumbhar,[‡] Jibao He,[§] Narayan Chandra Das,[||] Kaikun Yang,[||] Jian-Qing Wang,[⊥] Howard Wang,[||] Kevin L. Stokes,[#] and Jiye Fang*[,†]

Department of Chemistry, State University of New York at Binghamton, Binghamton, New York 13902, Electron Microscope Facility, Clemson University, Anderson, South Carolina 29625, Coordinated Instrumentation Facility, Tulane University, New Orleans, Louisiana 70118, Department of Mechanical Engineering, State University of New York at Binghamton, Binghamton, New York 13902, Department of Physics, State University of New York at Binghamton, Binghamton, New York 13902, and Department of Physics, University of New Orleans, New Orleans, Louisiana 70148

Received August 4, 2008; E-mail: jfang@binghamton.edu

Abstract: We report a preparation of high-quality cubic PbTe nanocrystals and their assembly into both square-array, two-dimensional patterns and three-dimensional simple cubic super crystals. The influence of oleylamine in the nanocrystal synthesis and core−shell formation through an anion-exchange mechanism was also studied. The simple cubic super crystals together with two-dimensional assembly patterns containing PbTe nanocubes and their core−shell building blocks were examined using TEM, SEM, AFM, XRD, SAXS, and FTIR. Such super crystals consisting of cubic structural building blocks may allow engineering of more complex materials from which novel properties may emerge.

Introduction

The super crystal (SC),[1−3] that is, three-dimensional (3D) self-assembly of a nanocrystal (NC) superlattice, has attracted increasing attention. However, the fabrication of an SC has remained a challenge and requires high-quality NC uniform in both size and shape. For identical spheres, both the hexagonal close-packing and the cubic close-packing give the highest packing efficiency, 74.04%. NCs used as building blocks could be present in various nonspherical shapes such as octahedrons[4] and cubes; in fact, an SC containing cubic NCs can achieve a packing density as high as 100% if the interparticle spacing is neglected. Although previous studies on two-dimensional (2D) ordered structures of cubic NCs indicate that formation of a square array is energetically more favorable than other close-packed arrangements such as a quasi-hexagonal array,[5] there have been very few reports that describe the manipulation and analysis of 3D SCs containing the building blocks of cubic NCs.[6,7] In general, a combination of structure-defined NC and long-range order assembly could offer unique electronic and optical properties. Here, we demonstrate our recent observation and analysis of simple cubic SCs containing PbTe nanocubes and their core−shell building blocks, PbTe@$Pb(OH)_2$ and PbTe@PbO, in size of ∼15 nm.

Experimental Section

Preparation of Monodisperse Cubic PbTe NCs. The fabrication of cubic PbTe NCs is based on our previous wet-chemical approach[8] with improved processing control. Such NCs can be further assembled into monolayer or multilayers on a copper grid or on a silicon wafer (or other film) with different packing densities by tuning a number of processing factors such as the NC concentration and the rate of solvent evaporation (detailed below). In a typical experiment, 0.5 mmol of lead acetate trihydrate (99.99+%), 1.0 mL of oleic acid (90%), and 10 mL of oleylamine (70%) were loaded into a three-neck round-bottom flask equipped with a condenser and attached to a Schlenk line under an argon stream. The mixture was heated to 200 °C with vigorous stirring. Once a clear light-yellow solution was formed, 0.5 mL of pre-prepared triocylphosphine (90%) telluride[8] (99.999%) (1.0 M for Te) was rapidly injected into the system. The reaction was then ceased 1 min after the injection by promptly replacing the heating source with a cold water bath.[9] The resultant NCs were isolated

[†] Department of Chemistry, State University of New York at Binghamton.
[‡] Clemson University. Present address: CHANL Instrumentation Facility, Institute for Advanced Materials, NanoScience and Technology, University of North Carolina at Chapel Hill, Chapel Hill, NC 27599-3216.
[§] Tulane University.
[||] Department of Mechanical Engineering, State University of New York at Binghamton.
[⊥] Department of Physics, State University of New York at Binghamton.
[#] University of New Orleans.

(1) Shevchenko, E. V.; Talapin, D. V.; Kotov, N. A.; O'Brien, S.; Murray, C. B. *Nature* **2006**, *439*, 55–59.
(2) Desvaux, C.; Amiens, C.; Fejes, P.; Renaud, P.; Respaud, M.; Lecante, P.; Snoeck, E.; Chaudret, B. *Nat. Mater.* **2005**, *4*, 750–753.
(3) Redi, F. X.; Cho, K.-S.; Murray, C. B.; O'Brien, S. *Nature* **2003**, *423*, 968–971.
(4) Lu, W.; Liu, Q.; Sun, Z.; He, J.; Ezeolu, C.; Fang, J. *J. Am. Chem. Soc.* **2008**, *130*, 6983–6991.
(5) Yamamuro, S.; Sumiyama, K. *Chem. Phys. Lett.* **2006**, *418*, 166–169.
(6) Li, F.; Delo, S. A.; Stein, A. *Angew. Chem., Int. Ed.* **2007**, *46*, 6666–6669.
(7) Dumestre, F.; Chaudret, B.; Amiens, C.; Renaud, P.; Fejes, P. *Science* **2004**, *303*, 821–823.
(8) Lu, W.; Fang, J.; Stokes, K. L.; Lin, J. *J. Am. Chem. Soc.* **2004**, *126*, 11798–11799.
(9) Caution: To deal with this hot solution, proper gloves should be worn and special care should be taken.

by precipitating the nanoparticles from the reaction system using a sufficient amount of ethyl alcohol (200 proof, AAPER) followed by centrifugation. Highly monodisperse PbTe nanocubes could be obtained after a standard size-selection post-treatment using a pair-solvent mixture of ethyl alcohol and anhydrous hexane (98.5%, BDH). After removal of oleylamine residue by repeated washing/centrifugation, the high-quality PbTe nanocubes could be redispersed into anhydrous hexane or tetrachloroethylene (99+%) as stock suspensions for use in the self-assembly studies. About 1% (vol) of oleic acid was introduced into the stock suspensions to protect the nanocubes against any further surface reactions as function of time. All of the chemicals mentioned above were purchased from Sigma-Aldrich and used as received, except those specified.

Formation of Nanocubic Composites. Instead of oleic acid, about 1% (vol) of oleylamine was added into the stock suspensions of freshly prepared PbTe nanocubes to create core−shell nanocubes. The sample was typically kept at room temperature for 20−30 days to allow partial conversion from PbTe to PbTe@$Pb(OH)_2$ through an OH^--Te^{2-} anionic exchange. The PbTe@$Pb(OH)_2$ core−shell nanocubes can be further transformed into PbTe@PbO core−shell nanocubes by a quick annealing of the samples deposited on a silicon substrate in a Lindberg/Blue tube furnace (TF55035A-1) at 200 °C for 5 min. Thermogravimetric analysis (TGA) was also conducted to monitor the decomposition of the $Pb(OH)_2$ shell.

Self-Assembly of Nanocubes. On a copper grid coated with Formvar/carbon (product code: 01801, from Ted Pella Inc.), nanocubes could be assembled via two pathways, designated as "fast" and "slow". For the fast process, the grid was horizontally placed on a piece of filter paper so that the excess solvent was rapidly absorbed by the paper as soon as the nanocube suspension was dropped using a pipet, leaving the NCs deposited on the grid. For the slow process, the grid was vertically hung by a pair of self-closing TEM tweezers and submerged in a suspension of PbTe nanocubes in a vial. The solvent was allowed to naturally evaporate until the level of the colloidal solution was below the TEM grid. In this way, NCs were slowly deposited on the grid at the interface of the solvent surface, TEM grid surface, and air. It should be pointed out that the concentration of the nanocube suspension is an additional factor that controls the quality of assembled pattern. SC of various nanocubes could also be built on a solid substrate, such as a silicon wafer or kapton film. Typically, a sufficient amount of concentrated nanocube suspension was prepared using 95 wt % of anhydrous hexane and 5 wt % of anhydrous ethanol. This colloidal suspension was transferred into a vial containing a piece of substrate horizontally placed on the bottom. The system was placed in an ambient environment until all of the solvent evaporated "naturally", leaving the nanocubes assembled onto the surface of the substrate.

Structural Analysis. Transmission electron microscopes (TEM, Hitachi 7600 and 9500, HD 2000) were used to image the structure of nanocubes and assemblies. Field emission scanning electron microscopes (FESEM, Hitachi S-4800 and Carl Zeiss Supra 55VP) were employed to investigate the morphology and structure of SCs. Atomic force microscopy (AFM) image was taken on a Digital Instruments Multimode/Nanoscope V scanning probe microscope in the tapping mode under ambient environment. Phase development was characterized using an X-ray diffractometer (XRD, PANalytical X-pert system with a Cu $K\alpha_1$ radiation). Small angle X-ray scattering (SAXS) patterns of PbTe nanocube suspensions and PbTe, PbTe@$Pb(OH)_2$ nanocube SCs were recorded at room temperature with Cu $K\alpha$ radiation from a 1.2 kW rotating anode X-ray generator (007 HF, Rigaku Denki Co. Ltd., Japan), and two-dimensional multiwire detector. The sample−detector distance of 1.5 m allowed a q range from 0.006 to 0.11 $Å^{-1}$ [$q = 4\pi/\lambda \sin(\theta/2)$, where λ is X-ray wavelength and θ is scattering angle]. The scattering intensity after subtraction of the empty cell scattering and background was circularly averaged. Near-IR optical absorption was observed on a Thermo Nicolet Nexus 670 FT-IR spectrometer using a pair of IR sample cells. White light was selected as the light source, and the hydrocarbon residue in the NC suspensions was removed by several cycles of flocculation−dispersion treatment before redispersing the nanocube precipitate into tetrachloroethylene.

Results and Discussion

A typical transmission electron microscopy (TEM) image of the fast-processed assembly[10] is presented in Figure 1a, showing that PbTe NCs of monolayer are close-packed into square arrays in short range with some uncovered areas. In contrast, we have also prepared a large-area assembly of monolayer NCs on a copper grid with high packing density using a slow process technique.[11] As an example, a TEM image in Figure 1b exhibits a pattern with square-ordered structure that was achieved through this "slow-process" pathway.[11] Figure 1c is a selected area electron diffraction (SAED) pattern of this high packing density monolayer assembly under projection direction of ⟨100⟩, for which more than 50 NCs were included. A repreparation of a TEM sample using concentrated PbTe NC suspensions (twice more concentrated than the original colloidal suspensions) through the "fast process" generated a multilayer pattern as shown in Figure 1d. It is worth mentioning that the success of an SC assembly is dependent on the fabrication of high-quality NCs with tight size distribution and controlled shape. Figure 1g demonstrates a high-resolution TEM (HRTEM) image of a PbTe NC, the building block of SC, indicating a well-evolved cubic shape and its {100} surfaces.

As illustrated in Figure 1d, the multilayer pattern is composed of many nanocube subarrays, each of which consists of ∼50−100 cubic NCs as shown in the inset of Figure 1d. We focus on TEM images of these subarrays and further analyze their packing structures. As discussed previously, for nanocubes, a simple cubic packing pattern will result in a 100% packing density theoretically and should be energetically favorable.[5] Because random sliding of face-to-face attached NC rows along the row direction in square array would result in no change in packing density, there could be at least three possible packing structures when the second layer of PbTe NCs is stacked on the top of the first layer: (a) exactly on top of each other (Figure 1e); (b) shifting along one axis in the horizontal plane (Figure 1f); and (c) shifting along two axes in the horizontal plane. We designate these three circumstances as "simple cubic SC", "1D-shifted SC", and "2D-shifted SC", respectively. On the basis of our TEM investigation, we have observed multilayered structures of "simple cubic SC" (Figure 1h) and "1D-shifted SC" (Figure 1i), indeed. We have also realized that the chance of determining "simple cubic SC" structure (illustrated in Figure 1e and h) is much higher than that of "1D-shifted SC" (illustrated in Figure 1f and i). No structure of "2D-shifted SC" (i.e., structure c) has been observed to date. In the structure of "simple cubic SC", the second layer of nanocubes is exactly

(10) A fast-processed TEM sample was prepared by casting a drop of cubic NC suspensions in anhydrous hexane onto a copper grid coated with Formvar/carbon (product code: 01801, from Ted Pella Inc.) at room temperature. The grid was horizontally placed on a piece of filter paper so that the solvent was absorbed by the paper as soon as the suspension was dropped, leaving the NCs deposited on the grid.

(11) The slow process for creating TEM samples can be described as follows: A copper grid coated with Formvar/carbon (product code: 01801, from Ted Pella Inc.) was vertically hung by a pair of self-closing TEM tweezers and submerged in a suspension of PbTe nanocubes in a vial. The concentration of the nanocube suspension is the same as that in the fast process. A large-area, monolayer assembly of NCs is slowly deposited on the grid as the solvent evaporates.

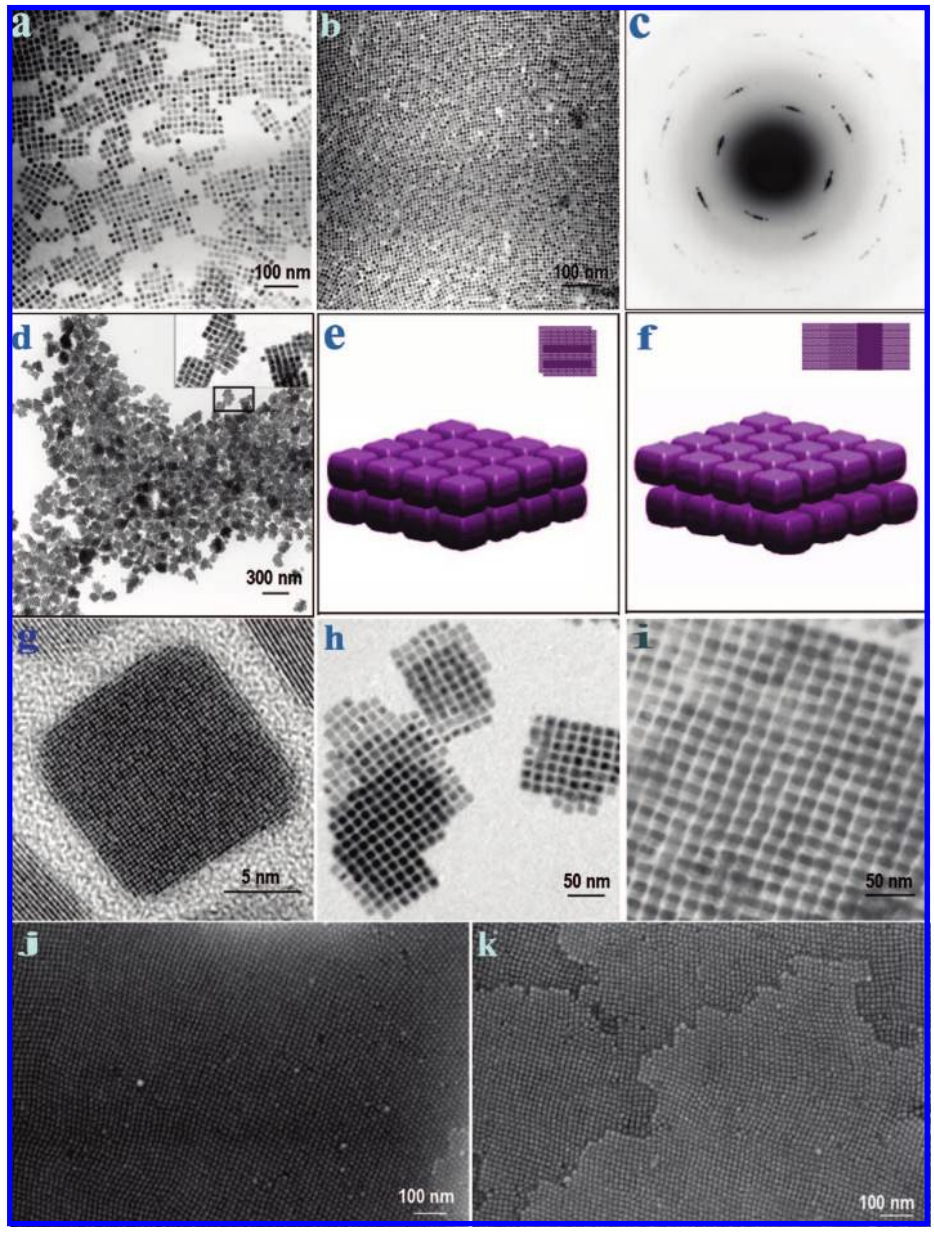

Figure 1. EM images of PbTe nanocubes and SC. (a) TEM image of fast-processed PbTe monolayer assemblies. (b) TEM image of slow-processed PbTe monolayer assembly. (c) Selected area electron diffraction pattern of slow-processed monolayer assembly (negative pattern). (d) TEM image of slow-processed PbTe multilayer assemblies. (e) Model of stacking structure of two-layer assembly: "simple cubic SC". (f) Model of stacking structure of two-layer assembly: "1D-shifted SC". (g) HRTEM image of a PbTe nanocube. (h) TEM image of "simple cubic SC" stacking structure: each nanocube is exactly stacked on the top of another. (i) TEM image of "1D-shifted SC" stacking structure: the top layer is shifted by half a length of the cubic edge along one axis. (j) FE-SEM image of PbTe simple cubic SC on an Si wafer, showing a smooth and flat surface in most areas except the edge region, which is presented in (k).

stacked on top of the bottom layer by maximally contacting the {100} surfaces of two adjacent facets, leading to a minimum of total surface energy. Therefore, as observed, this type of assembly should dominate the packing structures. We were also able to prepare quasi-monolayered PbTe nanocube assemblies and multilayered cubic PbTe SCs with characteristic dimensions on the order of micrometers. These assemblies were formed on a Cu grid via a TEM slow process pathway[11] and on a silicon wafer via an SEM slow process pathway[12] at room temperature (Figure S1 in the Supporting Information). As illustrated in Figure 1j and k, field-emission scanning electron microscopic analysis (FE-SEM) reveals that the top surface of the SC is flat, dense, and sufficiently large, at least on the order of tens of micrometers. Looking down along the vertical direction perpendicular to the wafer surface, Figure 1k also shows a structural characteristic of "simple cubic SC" (also refer to the inset of Figure S1b in the Supporting Information).

Concerning the formation of SC from PbTe nanocubes, we realize that the coordination of the organic capping ligand is one of the key factors. When oleic acid together with trioctylphosphine (TOP) were used as capping ligands in the original synthesis procedure (phenyl ether reaction medium),[8]

(12) A sufficient amount of concentrated PbTe nanocube suspension was transferred into a vial containing a piece of Si wafer placed horizontally on the bottom. The system was placed in an ambient environment, and the solvent (95 wt % of anhydrous hexane/5 wt % of anhydrous ethanol) was allowed to evaporate naturally, leaving a PbTe SC deposited onto the surface of the wafer.

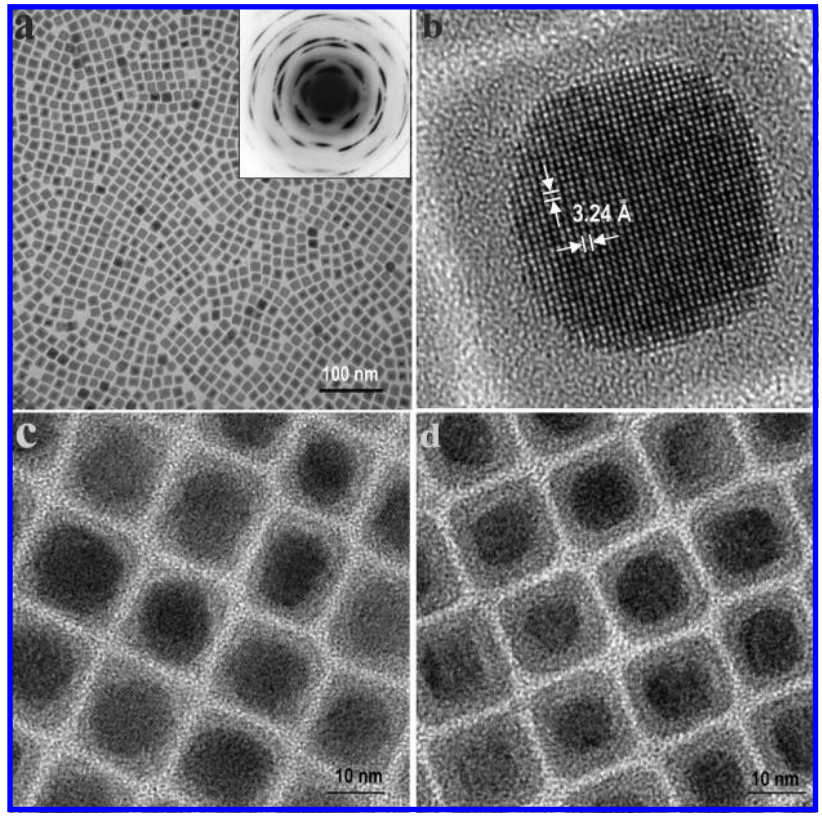

Figure 2. TEM images of PbTe@$Pb(OH)_2$ core−shell nanocube monolayer assembly. (a) Low-magnification TEM image (the inset is a negative pattern of SAED). (b) HRTEM image showing the structure of a core−shell particle. (c) High-magnification TEM image showing core−shell nanocubes with an average minimum shell thickness of ∼1.5 nm. (d) High-magnification TEM image showing core−shell nanocubes with an average minimum shell thickness of ∼2.5 nm.

for instance, PbTe nanocubes resulted when the colloidal system was aged at 200 °C for a long period of time. However, no SC was achieved with these PbTe NCs. If the oleic acid was partially replaced with oleylamine, we were able to produce well-developed PbTe nanocubes with a much shorter reaction time (∼40 s) for the same temperature. More importantly, only a combination of oleic acid and oleylamine could result in a formation of SC as described above. Soulantica et al. also reported that large SC built by Sn NCs could be prepared in an organic system consisting of an acid and its conjugated base.[13] It is well known that NCs could be stabilized in a nonpolar colloidal system if they were capped by certain organic molecules, which are normally slightly polar.[1,14] In the PbTe system, capping of oleic acid on PbTe nanocubes may enhance the repulsive potential among NCs because of the same type of charge on NCs imparted by oleic acid,[1] which is traditionally a proton donor and possesses a dipole moment. When a combination of oleylamine and oleic acid is employed in the reaction, we propose that the electrical charge carried on PbTe NCs should be reduced through a dynamic proton-transfer interaction[2,13] between the capped oleic acid and the "free" oleylamine molecules in solution, which presents in a relatively dominative amount and acts as a "buffer solution". This would weaken the repulsive force among NCs, minimizing the total surface energy when the (100) face and (100) face from two adjacent PbTe nanocubes maximally contacted each other.

Not only does oleylamine induce the formation of PbTe SC, but it can also convert the surface of PbTe nanocubes into $Pb(OH)_2$ or lead oxide. If no further treatment is involved to remove the excessive oleylamine from the surfaces of freshly prepared PbTe nanocubes after the PbTe NC synthesis, as described in the experimental section, the Te^{2-} in PbTe nanocubes can be partially replaced by OH^- from the trace amount of water in the alcohol. This reaction is facilitated by the presence of oleylamine and first produces a shell of amorphous $Pb(OH)_2$. The shell subsequently transforms to crystalline PbO after an annealing treatment while retaining the cubic particle shape. Figure 2a shows a TEM image of 2D pattern of PbTe@$Pb(OH)_2$ core−shell nanocubes prepared through the "slow-process" pathway,[11] whereas the TEM images of large-area 2D assembly consisting of PbTe@$Pb(OH)_2$ nanocubes can be found in Figure S2 in the Supporting Information. The SAED patterns as indicated both in the inset of Figure 2a and in Figure 1c demonstrate a rock-salt single-crystal structure of PbTe oriented along ⟨100⟩, implying low crystallinity of the shell portion. HRTEM image displayed in Figure 2b further verifies the amorphous structure of the shell and single-crystal structure of PbTe in the core with a lattice *d*-spacing of ∼3.24 Å, which corresponds to the {200} lattice planes of PbTe. The thickness of the shell can also be tuned by varying the length of the PbTe−$Pb(OH)_2$ conversion time. For example, PbTe@$Pb(OH)_2$ core−shell nanocubes with average minimum shell thicknesses[15] of ∼1.5 nm (Figure 2c) and ∼2.5 nm (Figure 2d) were prepared by adding a mixture of extra oleic

(13) Soulantica, K.; Maisonnat, A.; Fromen, M.-C.; Casanove, M.-J.; Chaudret, B. *Angew. Chem., Int. Ed.* **2003**, *42*, 1945–1949.
(14) Chen, Z.; O'Brien, S. *ACS Nano* **2008**, *2*, 1219–1229.

Scheme 1. Mechanism Illustration of PbTe Nanocube Hydrolysis[a]

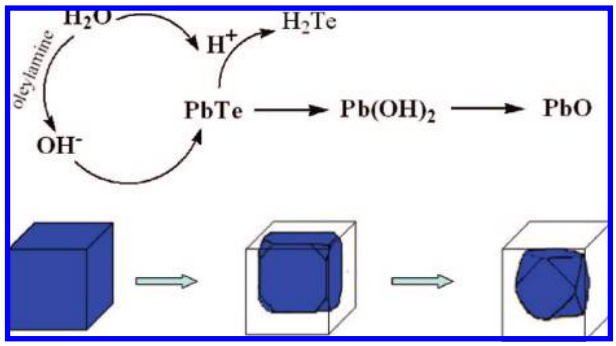

[a] Top: Schematic illustration of anion-exchange involved in the conversion of PbTe to $Pb(OH)_2$. Bottom: Schematic illustration of shape-evolution of a PbTe nanocube during the hydrolysis to $Pb(OH)_2$.

acid and alcohol into the systems "aged" for 20 days and 30 days, respectively, to stop the oleylamine-induced conversion.

As proposed in Scheme 1, it is believed that the surface of PbTe nanocubes could be slowly converted to amorphous $Pb(OH)_2$, in the presence of oleylamine as a catalyst through an anion-exchange mechanism, and the resultant $Pb(OH)_2$ shells could further be decomposed to PbO after an annealing treatment (refer to the XRD investigation). As illustrated in Scheme 1 and Figure 2c,d, it is believed that the anion-replacement reaction initiates from the corners of PbTe nanocubes due to their higher surface energy instead of other location on the surfaces. This leads to an exposition of {111} faces of PbTe nanocubes, evolving the shape of the PbTe core from truncated cube with low ratio of {111}/{100} to truncated octahedron with high ratio of {111}/{100}.[16] Eventually, truncated octahedral or nearly spherical PbTe core could be developed while the exterior cubic shape of the entire NC was preserved. We therefore infer that anion-exchange rates on various positions on surface of a PbTe nanocube are different depending on its crystallography planes, and reaction in ⟨111⟩ direction should dominate the PbTe−nanocube transformation. Because the as-formed $Pb(OH)_2$ shells are amorphous and slightly altered to truncated nanocubes in shape, close-packed 2D assembly pattern of the core−shell nanocubes would no longer present square-array structure as displayed in Figures 2a and S2. This can actually be verified by a comparison of SAED patterns between Figure 1c and the insert of Figure 2a as well, implying that the assembly pattern of PbTe nanocubes should possess higher long-range order than that of the core−shell nanocubes. Furthermore, the optical behavior of IV−VI semiconductors is interesting due to the strong confinement on their electrons and phonons.[17,18] As expected, the optical characteristic of PbTe nanocubes may be altered when a layer of $Pb(OH)_2$ was formed on the surface. As depicted in Figure S3a in the Supporting Information, ∼14 nm PbTe shows near-IR absorption peaks ranged at ∼4335 and ∼4080 cm^{-1}, which is comparable to the reported result of 8.8 nm PbTe nanocrystals[19] after a suitable size-effect correction.[20] Figure S3b displays the spectrum after the introduction of $Pb(OH)_2$ layer on the PbTe nanocubes (anion-exchange for 20 days), revealing that the two above-mentioned peaks on the spectrum of the core−shell nanocubes have "blue-shifted" (toward increasing wavenumber) by ∼85 cm^{-1} due to the smaller PbTe core after the shell was formed. In Figure S3b in the Supporting Information, not only do the peaks at both 4420 and 4165 cm^{-1} "blue-shift" by ∼85 cm^{-1}, but the second group of peaks ranged in 4165 and 4120 cm^{-1} also obviously intensity-enhances due to a number of complicated reasons, possibly including the type-I core−shell effect.[21−23]

It is necessary to emphasize that such PbTe@$Pb(OH)_2$ core−shell nanocubes can also be packed into an SC on an Si wafer or on a kapton film using a slow-processing approach.[12] To identify the structure of this PbTe@$Pb(OH)_2$ SC, we have carried out a small-angle X-ray scattering (SAXS) study on kapton-supported PbTe@$Pb(OH)_2$ SC, kapton-supported PbTe SC, as well as the PbTe suspensions in hexane for comparison. In SAXS, the total scattering intensity should be proportional to the number of objects, the structure factor that describes how the objects are arranged in space, and the form factor that describes the electron density distribution of an individual object or primary NC. The data are presented as a function of scattering vector, q, which is related to the scattering angle as given above. The characteristic q at the peak intensity is inversely proportional to D, the mesoscopic lattice spacing. Figure 3a reveals reflections arising from the scattering of X-rays off the planes of the nanocube SCs.[24] Plotting the indexed curves in Figure 3a reveals that both the PbTe SC and the PbTe@$Pb(OH)_2$ SC are preferentially (100)-oriented with respect to the substrate surfaces such as (200), (300), etc. This confirms that both types of SCs should be simple cubic superlattices as imaged in TEM and SEM. In comparison with the SAXS curve of PbTe SC, the slight peak shift toward smaller q (i.e., larger D) in the curve of the PbTe@$Pb(OH)_2$ SC indicates an increase of intercore distance in the SC due to the formation of amorphous $Pb(OH)_2$ layer and the simultaneous shrinking of the crystalline PbTe core. In contrast, Figure 3b presents a SAXS spectrum of PbTe nanocube suspensions in hexane and the best model fitting (solid curve through symbols) using the cubic form factor only, implying complete dispersion of nanocubes in hexane. The fitting shows an average size of ∼13 ± 2 nm, which is in agreement with the TEM observation.

We also annealed the Si-wafer-supported core−shell SC fabricated with cubic PbTe@$Pb(OH)_2$ for 5 min at 200 °C to convert the $Pb(OH)_2$ shell to PbO.[25] These annealed structures still retained simple cubic packing as shown in Figure 4a,b. The only observable difference between Figure 4a and Figure 1j and k is that the former possesses some "cracks" in large-scaled observation zone, which is from shrinkage due to the thermal decomposition of $Pb(OH)_2$ while being heated. Phase AFM

(15) Minimum shell thickness means a thickness measured from a center point of a cube face on the shell to the closest point on the surface of the core.
(16) Wang, Z. L. *J. Phys. Chem. B* **2000**, *104*, 1153–1175.
(17) Wise, F. W. *Acc. Chem. Res.* **2000**, *33*, 773–780.
(18) Tudury, G. E.; Marquezini, M. V.; Ferreira, L. G.; Barbosa, L. C.; Cesar, C. L. *Phys. Rev. B* **2000**, *62*, 7357–7364.
(19) Urban, J. J.; Talapin, D. V.; Shevchenko, E. V.; Murray, C. B. *J. Am. Chem. Soc.* **2006**, *128*, 3248–3255.
(20) The relationship between wavenumber (W in cm^{-1}) and wavelength (λ in nm) is $W = 10^7/\lambda$. Two wavelengths of the absorption peaks from 8.8 nm PbTe from the literature can be roughly converted to wavenumbers of 4940 and 4430 cm^{-1}.
(21) Peng, X.; Schlamp, M. C.; Kadavanich, A. V.; Alivisatos, A. P. *J. Am. Chem. Soc.* **1997**, *119*, 7019–7029.
(22) Dabbousi, B. O.; Rodriguez-Viejo, J.; Mikulec, F. V.; Heine, J. R.; Mattoussi, H.; Ober, R.; Jensen, K. F.; Bawendi, M. G. *J. Phys. Chem. B* **1997**, *101*, 9463–9475.
(23) Mii, O. I.; Smith, B. B.; Nozik, A. J. *J. Phys. Chem. B* **2000**, *104*, 12149–12156.
(24) Murray, C. B.; Kagan, C. R.; Bawendi, M. G. *Annu. Rev. Mater. Sci.* **2000**, *30*, 545–610.
(25) TGA investigation indicated that decomposition of the $Pb(OH)_2$ shell occurs at ∼180 °C.

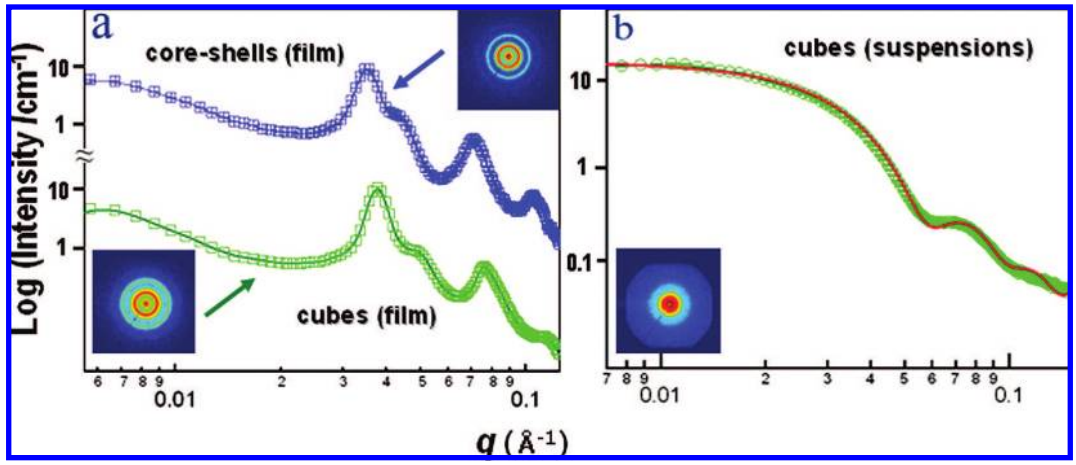

Figure 3. SAXS patterns (inset) and corresponding radial-averaged spectra for (a) PbTe SC (thin film, labeled as "cubes") and PbTe@$Pb(OH)_2$ SC (thin film, labeled as "core−shells") assembled on kapton films and (b) PbTe nanocube suspensions in hexane.

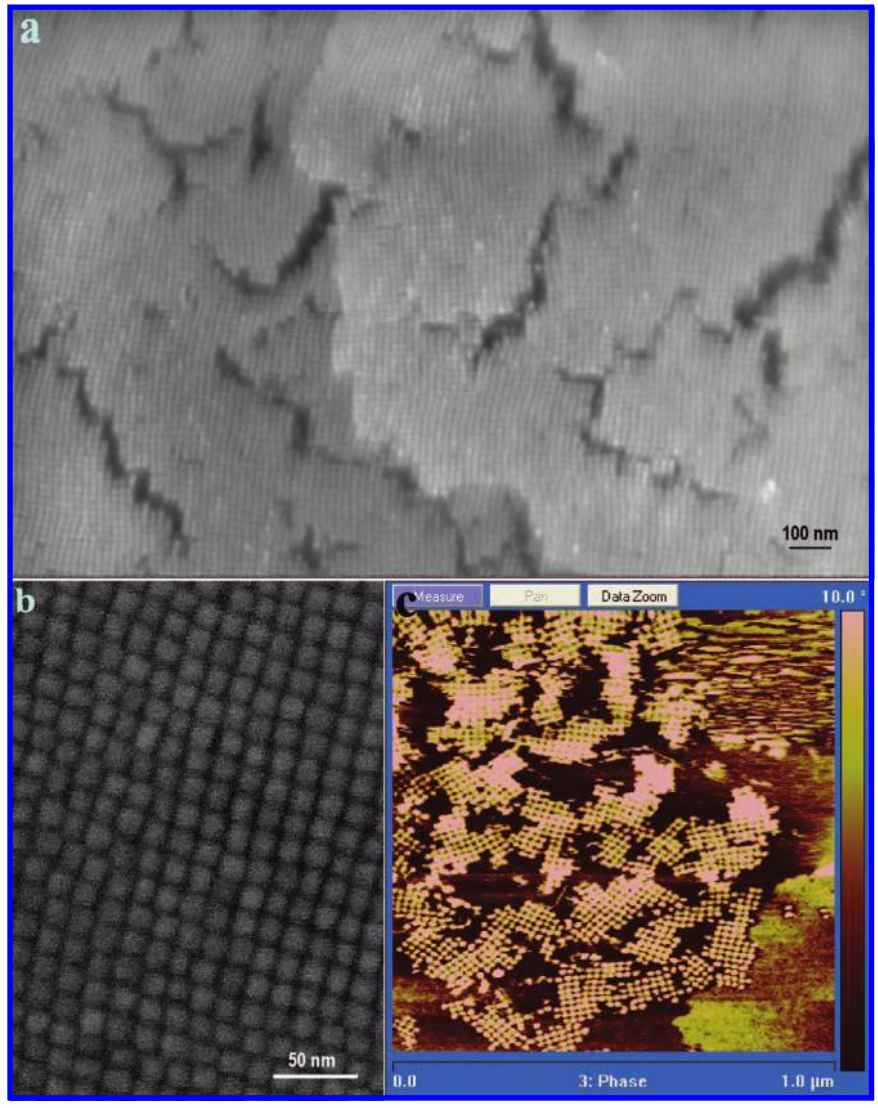

Figure 4. SEM and AFM images of PbTe@PbO single-cubic SC. Sample was achieved by first assembing PbTe@$Pb(OH)_2$ nanocubes on a Si wafer through a "slow processing" and then annealing at 200 °C for 5 min in a tube furnace under argon stream. (a) FE-SEM image. (b) High resolution of SEM image. (c) AFM image.

image (Figure 4c) confirms the "broken" packing structures on the nanocube surface layers. To further monitor the phase development, we have alternatively recorded their X-ray diffraction (XRD) patterns of PbTe, PbTe@$Pb(OH)_2$, and PbTe@PbO nanocubes, respectively. In the XRD trace of PbTe nanocubes (Figure 5a), highly crystalline fcc PbTe structure with the *Fm*3*m*

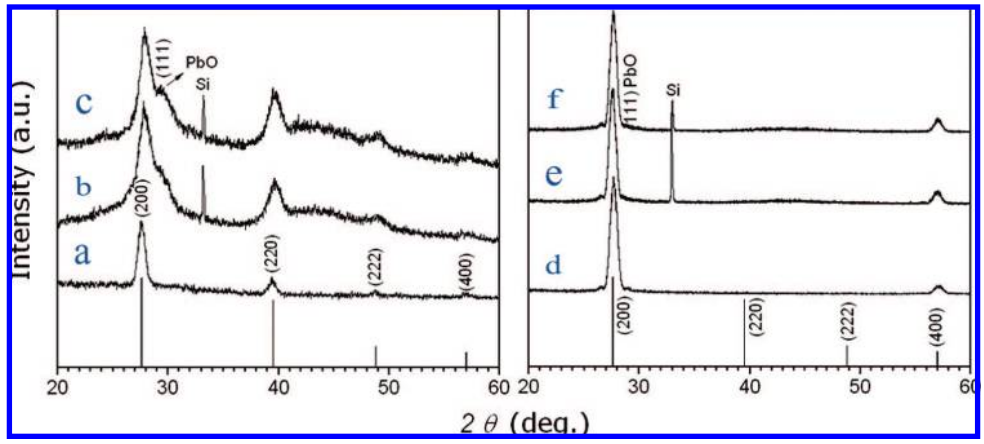

Figure 5. XRD patterns of PbTe and core−shell nanocubes. (a−c) Samples were randomly deposited on a PANalytical Si zero background sample holder; (d−f) samples were assembled on a polished 25 mm Si ⟨100⟩ wafer. (a and d) XRD trace of PbTe nanocubes. (b and e) XRD trace of PbTe@$Pb(OH)_2$ core−shell nanocubes. (c and f) XRD trace of PbTe@PbO core−shell nanocubes (annealing of PbTe@$Pb(OH)_2$ core−shell nanocubes at 200 °C for 5 min).

space group could be detected, and all of the detected peaks are indexed as those from the standard ICDD PDF card (no. 38-1435). The formation of orthorhombic PbO (ICDD PDF card no. 76-1796) as a minor phase could be detected in the XRD trace of the annealed sample with a typical peak centered at 29.3° (Figure 5c), whereas the presence of $Pb(OH)_2$ phase in XRD trace shown in Figure 5b is not obvious most likely due to its amorphous state prior to heat treatment. It is worth noting that assemblies of the three above-mentioned samples on polished wafers could result in an apparent enhancement (more than 10 times) on peaks (200) and (400) of PbTe diffraction patterns and an absence of others such as (220) and (222) [Figure 4d−f]. As discussed previously,[8] this further verifies that all three types of samples assembled on surface of the polished Si wafer are perfect cubic in their external shape. Such great intensity-enhancement on diffraction (200) can even "overlap" with the (111) diffraction peak of PbO as shown in Figure 5f (note that patterns in Figure 5c and f were recorded from the same sample of PbTe@PbO nanocubes).

Conclusions

In conclusion, we have prepared high-quality cubic PbTe NCs and PbTe@PbO core−shell NC as well as their assembly into two-dimensional square-arrays and three-dimensional simple cubic super crystals. Various characterizations including TEM, SEM, AFM, XRD, SAXS, and FTIR have been conducted to examine the nature of extended mesoscopic structures and potential properties. Analysis of these structures reveals that oleylamine as a conjugated base plays a very important role in the self-assembly process. Through an anion-exchange mechanism in the presence of oleylamine, such PbTe nanocube can be further converted into a core−shell building block by "shrinking" itself into a truncated octahedral or nearly spherical core with an amorphous but quasi-cubic shell (PbTe@$Pb(OH)_2$ and PbTe@PbO). The cubic core−shell particles can still be packed into a 2D pattern or a super crystal, but the long-range order was lost due to a slight truncation of the corners of the NCs. Not only is the super crystal itself of sufficient interest, but the combination of such structured cubic building blocks and long-range ordered assembly could result in unique applications in electronic or photonic devices.

Acknowledgment. This work was supported by the NSF CAREER program (DMR-0731382), ADL, and State University of New York at Binghamton.

Supporting Information Available: TEM images of quasi-monolayered PbTe nanocube assembly in scale of micrometers; SEM image of PbTe nanocube SC in scale of micrometers; TEM image of large-area 2D PbTe@$Pb(OH)_2$ nanocube self-assembly; and near-IR absorption spectra of cubic PbTe NCs and PbTe@$Pb(OH)_2$ core−shell nanoparticles. This material is available free of charge via the Internet at http://pubs.acs.org.

JA806120W